Metaplastic tuft cells transdifferentiate to neural-like progenitor cells in the progression of pancreatic cancer

Daniel J. Salas-Escabillas[1,2]; Megan T. Hoffman, PhD[3]; Jacee S. Moore, MS[2]; Sydney M. Brender, MS[2]; Hui-Ju Wen, PhD[2]; Simone Benitz, PhD[2]; Erick T. Davis[2]; Dan Long[2]; Allison M. Wombwell[2]; Nina G. Steele, PhD[2]; Rosalie C. Sears, PhD[4]; Ichiro Matsumoto, PhD[5]; Kathleen E. DelGiorno, PhD[6]; Howard C. Crawford, PhD* [2, 7]

[1] Cancer Biology, University of Michigan, Ann Arbor, MI

[2]Henry Ford Pancreatic Cancer Center, Henry Ford Health, Detroit, MI

[3]Dana-Farber Cancer Institute, Harvard Medical School, Boston, MA

[4]Oregon Health & Science University, Portland, OR

[5]Monell Chemical Senses Center, Philadelphia, PA

[6]Vanderbilt University School of Medicine, Nashville, TN

[7]Wayne State University, Detroit, MI

*Corresponding Author:

Howard C. Crawford, PhD, Department of Surgery, Henry Ford Health System, Detroit, Michigan, USA

Email: hcrawfo1@hfhs.org

Abstract

Background: Pancreatic cancer is partly derived from the transdifferentiation of acinar cells into metaplastic ducts that act as precursors of neoplasia and cancer. Tuft cells are solitary chemosensory cells not found in the normal pancreas but arise in metaplasia and neoplasia, gradually disappearing as neoplastic lesions progress to carcinoma. Metaplastic tuft cells (mTCs) functionally suppress tumor progression through communication with the tumor microenvironment, but their fate during progression is unknown.

Methods: To determine the fate of mTCs during PDA progression, we have created a lineage tracing model that uses a tamoxifen-inducible tuft-cell specific Pou2f3$^{CreERT/+}$ driver to induce transgene expression, including the lineage tracer tdTomato or cMyc. FlpO-driven, mTC lineage trace models of pancreatic neoplasia (Ptf1a$^{FlpO/+}$; FSF-KRAS$^{G12D/+}$; Pou2f3$^{CreERT/+}$; ROSA26$^{LSL\text{-}TdTomato/+}$, "*KF-P2f3T*") and carcinoma (Ptf1a$^{FlpO/+}$; FSF-KRAS$^{G12D/+}$; Trp53$^{Frt\text{-}Exons\ 2\ to\ 5\text{-}Frt/+}$; Pou2f3$^{CreERT/+}$; ROSA26$^{LSL\text{-}TdTomato/+}$, "*KPF-P2f3T*") were used to follow mTC fate. Co-immunofluorescence was used to determine the identity of lineage-traced cells throughout the progression of neoplasia and carcinoma.

Results: We found that mTCs, specifically in the KPF-P2f3T carcinoma model, transdifferentiate spontaneously into neural-like progenitor cells (NRPs), a cell type associated with poor survival in pancreatic cancer patients. This Tuft-to-Neuroendocrine Transition (TNT) does not occur in *KF-P2f3T* neoplasia until cMyc expression is targeted directly in mTCs.

Introduction

Pancreatic ductal adenocarcinoma (PDA), the most common form of pancreatic cancer, is a devastating disease with a 5-year survival rate of only 13% [1]. Effective treatment options are few, and reliable early detection methods needed to enhance treatment effectiveness are non-existent. PDA is initiated by oncogenic mutations in the *KRAS* gene, causing irreversible transdifferentiation of normal acinar cells into metaplastic ducts. Metaplastic ducts then progress to pancreatic intraepithelial neoplasia (PanIN) [2] and, with the acquisition of mutations in tumor suppressors such as *TP53*, *CDKN2A*, or *SMAD4* [3, 4], progress to invasive carcinoma. Metaplastic ducts are a heterogeneous population of reactive epithelial cells [5] comprised of at least 6 distinct identities: gastric neck cells [6], gastric pit-like cells, gastric chief-like cells, ductal senescent cells, metaplastic neuroendocrine cells (mNECs), and specialized chemosensory cells known as metaplastic tuft cells [7].

Normal tuft cells are solitary chemosensory cells found throughout the body that sense and respond to environmental cues to maintain tissue homeostasis. Functionally, they use the canonical gustatory signal transduction pathway, with specific stimulants and responses depending on context and the organ in which they reside [8-10]. In pancreatic neoplasia, metaplastic tuft cells (hereafter referred to as mTCs), have been proposed to be a class of tumor progenitor cell [9, 11], but functionally they suppress progression to PDA via inhibition of anti-inflammatory immune cells through crosstalk with the tumor microenvironment [8, 10]. mTCs are identified by staining for markers such as Acetylated-*Tuba1a*, *Dclk1*, *Vav1*, *Cox1*, *Cox2*, *Trpm5*, and *Pou2f3*, the latter being the master transcriptional regulator of tuft cell genesis [8, 12-15]. mTCs are not typically found in the normal pancreas and only appear after prolonged damage, such as in chronic pancreatitis [16] or the initiation of neoplasia [9, 11], arising from the transdifferentiation of acinar cells. As neoplasia progresses to invasive carcinoma,

the mTC population gradually disappears, challenging their putative role as classic tumor progenitor cells.

In the current study, to address the hypothesis that mTCs act as tumor progenitor cells in pancreatic cancer, we lineage-traced their fate during disease progression in mice. To accomplish this, we used a dual recombinase model wherein tumorigenesis is initiated by the expression of FlpO recombinase knocked into the pancreas-specific *Ptf1a* locus, driving the expression of an Frt-STOP-Frt oncogenic *Kras*$^{G12D/+}$ allele and the deletion an Frt-flanked allele of *Trp53* [17]. This model allowed us to use an inducible *Pou2f3*$^{CreERT/+}$ driver [18] to target the expression of a *ROSA26*$^{LSL\text{-}TdTomato}$ lineage trace reporter specifically to mTCs [14, 19] in both neoplasia and carcinoma, indelibly labeling mTCs and their progeny. In the *Ptf1a*$^{FlpO/+}$; *Kras*^{G12D} neoplasia model, mTCs and other metaplastic cellular subtypes, including neuroendocrine-like enteroendocrine cells [7, 20, 21] arise from acinar cells, independent from one another. However, in the *Ptf1a*$^{FlpO/+}$; *Kras*$^{FSF\text{-}G12D/+}$; *Trp53*$^{Frt\text{-}Exons\ 2\ to\ 5\text{-}Frt/+}$ carcinoma model, we found that acinar cell-derived mTCs transdifferentiate to neural-like progenitor cells (NRPs) [20], also known as ductal neuroendocrine cells [22]. NRPs in PDA patients correlate with worse survival, are resistant to chemotherapy, and their genesis is associated with elevated cMyc activity [20, 22]. Indeed, targeting the expression of cMyc to mTCs in *Ptf1a*$^{FlpO/+}$; *Kras*^{G12D} mice was sufficient to drive transdifferentiation of mTCs to NRPs.

RESULTS

Pou2f3-CreERT specifically targets metaplastic tuft cells in the pancreas

Tuft cells are not found in the normal mouse pancreas but arise from the transdifferentiation of acinar cells in conditions of tissue damage and early neoplasia [23]. As neoplasia progresses, metaplastic tuft cells (mTCs) decrease in number and are absent in carcinoma [9, 11, 23]. To determine the fate of mTCs during neoplastic progression, we developed a novel dual recombinase lineage trace system, wherein Ptf1a$^{Flpo/+}$ initiates expression of oncogenic Kras from a Kras$^{Frt\text{-}Stop\text{-}Frt\text{-}G12D}$ allele (*KF*) to drive neoplasia [17] (Fig. 1A, 1D). When combined with a conditional knockout trp53 allele with exons 2-5 flanked by Frt recombination sites (Trp53$^{Frt\text{-}Exons\ 2\ to\ 5\text{-}Frt/+}$), lesions rapidly progress from neoplasia to carcinoma (*KPF*) (Fig. 1B, 1D). Within this system, we introduced a Cre^{ERT} driver knocked into the *Pou2f3* locus [18], which encodes the transcription factor master regulator of tuft cell genesis [14, 15, 19, 24, 25]. *Pou2f3$^{CreERT/+}$* was used to drive recombination and expression of a *ROSA26R$^{LSL\text{-}tdTomato}$* reporter [26] in a tamoxifen-inducible manner (P2f3T) [8, 19, 25], allowing us to lineage trace mTCs temporally in our neoplasia (*KF-P2f3T)* and carcinoma (*KPF-P2f3T)* models.

To determine the fidelity of our systems in labeling tuft cells, we treated *KF-P2f3T* with cerulein at 8-9 weeks of age to induce mild pancreatitis and accelerate transformation, then allowed the mice to recover for 3 weeks to optimize mTC genesis [9, 11]. The *KPF-P2f3T* carcinoma model induced sufficient transformation and mTC formation at 11-12 weeks of age with no additional treatment (Fig. 1C). Cerulein-treated *KF-P2f3T* and 11–12-week-old *KPF-P2f3T* mice were treated with tamoxifen to induce tdTom reporter expression, and the pancreata harvested 1 day later. We co-stained tissues for tdTom and the tuft cell markers

Pou2f3, Acetylated-α-tubulin, Cox1, Dclk1, Trpm5, and Vav1 (Fig. 1E and Supp. Fig. 1A, 1B) by immunofluorescence (IF). In both models, we found co-expression of tdTom exclusively in cells expressing mTC markers (Supp. Fig. 1A, 1B), confirming the system's specificity and allowing us to trace mTC fate throughout the progression of PDA.

Metaplastic tuft cells change identity in a model of pancreatic adenocarcinoma

To determine the fate of the mTC population over time, we collected tissue from our *KF-P2f3T* and *KPF-P2f3T* mice 3 days and 7 weeks post-tamoxifen. In the *KF-P2f3T* neoplasia model, all tdTom$^+$ cells co-expressed tuft cell markers (Fig. 2A). The population of mTCs dropped off slightly over this period but largely remained stable (Fig. 2B, *Black*). In contrast, in the *KPF-P2f3T* carcinoma model, the mTC population dropped drastically by 7 weeks, consistent with their disappearance as PanIN progresses to PDA [9, 11] (Fig. 2A and 2B, *Black*). We found no evidence that mTC attrition was associated with apoptosis by co-staining for cleaved caspase 3 (CC3) (Fig. 1F). Instead, we noted that tdTom$^+$ cells persisted in this model but no longer expressed mTC markers (Fig. 2A), suggesting that mTCs take on a new cellular identity.

Quantitation of the tdTom expression throughout multiple pancreata revealed that, in the *KPF-P2f3T* carcinoma model, the Cox1$^+$ mTC population dropped from an average of 15% at 3 days post-tamoxifen to an average of 3% at 7 weeks post-tamoxifen (Fig. 2B, *Black*). In contrast, the mTC progeny population, defined as tdTom$^+$ cells not expressing Cox1, increased by ~5-fold from an average of 4% of pancreatic ducts at 3 days post-tamoxifen to an average of nearly 17% at 7 weeks post-tamoxifen, reflecting the degree of mTC loss (Fig. 2B, *Pink*). These data suggest that mTCs are not undergoing cell death but are adopting a new identity in the carcinoma model.

Transdifferentiation of mTCs to metaplastic neuroendocrine cells.

To investigate the identity of the mTC progeny, we co-stained for tdTom together with markers of the known identities of other metaplastic ductal cells defined by *Schlesinger et al*. and *Benitz et al.*, including gastric pit-like (Gkn1$^+$), gastric neck-like (Lectin GS-II$^+$)[27], and metaplastic neuroendocrine cells (Syp$^+$) [7].

The lack of co-expression of tdTom with Gkn1 or Lectin GS-II suggested that *KPF-P2f3T* tdTom$^+$ mTC progeny had not taken on gastric pit-like cell or gastric neck-like cell identities (Fig. 2C and Supp. Fig. 2A). Instead, mTC progeny stained positive for Syp, revealing the acquisition of a metaplastic neuroendocrine cell (mNEC) identity (Fig. 2C, *Yellow arrows*). To determine if tdTom expression in cells with a neuroendocrine phenotype could be due to previously unnoticed recombination in pancreatic islets, we confirmed no co-localization of tdTom co-staining with Insulin (INS) or in surrounding islet cells (Supp. Fig. 2B). Quantitation of the different time points for the *KPF-P2f3T* model confirmed a decrease of tdTom$^+$/Cox1$^+$ mTCs, (Fig. 2E, *Black*), with a concomitant ~4-fold increase of tdTom$^+$/Syp$^+$ mNECs, (Fig. 2E, *Pink*) by 7 weeks post-tamoxifen (Fig. 2D, 2E). Interestingly, while there is a mNEC population in the metaplastic ducts in the *KF-P2f3T* neoplasia model, none expressed tdTom, suggesting that they did not derive from mTCs (Fig. 2D, 2E, *Green*) and have a distinct origin from those in the *KPF-P2f3T* mice.

mNECs depend on the mTC population to develop in PDA but not PanIN models.

Lineage tracing experiments show that mNECs in both neoplasia and carcinoma models are initially derived from acinar cells [9] (Supp. Fig 2C) but differ in that carcinoma mNECs derive from an mTC intermediate. As an independent test of these divergent origins, we took advantage of our *Pou2f3*^{CreERT} driver being a knock-in to the *Pou2f3* allele, thus

inactivating endogenous Pou2f3 activity [19]. By creating a model homozygous for *Pou2f3*^{CreERT}, we effectively ablated *Pou2f3* (Supp. Fig. 3A, 3B), preventing mTC formation [8] and therefore, any mTC progeny. Consistent with our previous observations, Cox1^{+} mTC and Syp^{+} mNEC populations were easily identifiable in the pancreatic lesions of our KF; Pou2f3$^{CreERT/+}$ neoplasia model. Pou2f3 ablation in these mice eliminated the mTC population, as expected, while the mNEC population persisted (Fig. 3A), supporting their independent origins. In contrast, in the KPF; Pou2f3$^{CreERT/CreERT}$ carcinoma mice, we found neither mTCs nor mNECs, confirming a shared dependency on Pou2f3 function (Fig. 3A, *Green arrows*).

Lineage tracing and Pou2f3 ablation data in KPF mice support a model where mTCs give rise to mNECs. However, it was also possible that in the KPF model, both cell types express *Pou2f3* and require its activity. mNECs do not express *Pou2f3* in *Kras*^{G12D}-driven neoplasia [7, 21, 25] but have not been examined in the KPF carcinoma model. To address this, we performed co-immunofluorescence for Pou2f3, together with Cox1 (mTCs) and Syp (mNECs). As expected, Pou2f3 was readily detectable in mTCs in both KF and KPF pancreata (Fig 1E, 3B). In contrast, we found no examples of Pou2f3^{+} mNECs in either system (Fig. 3B). The lack of identifiable recombination in early mNECs suggests that increasing population of tdTom^{+} mNEC cells is dependent on the prior genesis of the mTC population.

mTCs transdifferentiate into mNECs in PDA.

The observation that mTCs act as a precursor cell to mNECs suggested two possible models for this relationship: mTCs act as a stem-like cell, giving rise to mNEC daughter cells, or alternatively they directly transdifferentiate to mNECs. To distinguish these possibilities,

we tested if mNEC genesis required cell division, consistent with them arising from an asymmetric cell division of mTCs. MTCs rarely proliferate in neoplasia models [28], but their proliferative capacity has not been examined in a carcinoma model.

Initially, we co-stained for Ki67 and Syp and found that, like mTCs, mNECs were not in cell cycle in *KF-P2f3T* or *KPF-P2f3T* mice (Fig. 3C, *Black arrows*). To test if a rare cell division event was necessary for mNEC genesis, we used a long-term EdU incorporation assay to determine if mNECs had gone through a prior cell division [9, 11]. *KPF-P2f3T* mice were treated with tamoxifen once daily for 5 days at 11-12 weeks of age. We treated mice with EdU every 12 hours for 3 days and collected pancreata 12 hours after the last injection. Although we identified several EdU+ cells in the tissue (*Magenta arrows)*, neither Cox1^{+} mTCs (*Green arrows)* nor Syp^{+} TNTs (*White arrows*) had incorporated EdU (Fig. 3D), and, given the relatively long-time frame to allow for incorporation, were unlikely to have proliferated prior to their appearance.

To test the alternative that mTC-derived mNECs arise from the direct transdifferentiation of mTCs, we hypothesized that there would be cells that exist in mid-transition, co-expressing markers of both mTCs (Cox1) and mNECs (Syp). To identify transitionary cells, we co-stained Cox1 and Syp in *KPF-P2f3T* mice at 7 weeks post-tamoxifen treatment. Although rare, we identified several cells expressing both Cox1 and Syp (Fig. 3E, *Yellow arrows*) exclusively in *KPF-P2f3T* mice. These transitionary cells were also EdU negative (Supp. Fig. 3C, *Yellow arrows*). Collectively, our data support a “Tuft-to-Neuroendocrine Transition” (TNT) transdifferentiation event, analogous to an epithelial-to-mesenchymal transition, exclusively in our pancreatic carcinoma model.

Neoplastic mNECs have an enteroendocrine phenotype

We have found mNECs in the pancreata of both neoplasia and carcinoma models, but which diverge in their cellular origins. mNECs in both models are derived from acinar cells [16, 21], but in the *KPF-P2f3T* carcinoma model, mNECs require the genesis of an mTC intermediate. This unexpected observation led us to ask if mNECs in the KF-P2f3T neoplasia model and the KPF-P2f3T carcinoma models are distinct identities.

Two types of mNECs have been described in human pancreatic disease: neuroendocrine-like cells [20] also known as enteroendocrine cells (EECs) [16, 21], marked by their expression of islet cell hormones, and neural-like progenitor cells (NRPs) [20], also called ductal neuroendocrine cells [7, 22], marked by the expression of genes associated with neural development . EECs are known to be separate from tuft cells in pancreatic disease progression [16, 21], do not rely on Pou2f3 activity [16, 21, 29], and express markers of normal islet cells [20, 21]. To determine if mNECs in our models bore an EEC phenotype, we examined islet cell hormone expression [20] by co-IF of wide-spectrum cytokeratin (PanCK) and Syp together with either glucagon (Gcg), insulin (Ins), somatostatin (Sst), pancreatic polypeptide (Pp), and ghrelin (Ghrl), markers of α, β, δ, γ, and ε islet cells, respectively [30].

Since the KF mNECs do not express a lineage tracer, we confined our analysis to PanCK$^+$/Syp$^+$ cells to distinguish them from singular islet cells that can become trapped within the diseased tissue (Figs. 4A-E & Supp. Fig. 3D). In the *KF-P2f3T* neoplasia model, we consistently found isolated mTC-independent mNECs expressing islet cell identity markers apart from the beta-cell markers Ins and serotonin (5-HT) (Fig. 4B and Supp. Fig. 2B). In contrast, we found no islet hormone expression in the mTC-derived mNECs in the *KPF-P2f3T* mouse. These data indicated that mNECs in our KF-P2f3T neoplasia model, but

not in our *KPF-P2f3T* carcinoma model, are likely EECs similar to those found in other models of pancreatic disease [16, 20, 21].

Cells derived from TNT persist in pancreatic carcinoma

Having established that mNECs in KF neoplasia are EECs, whereas those in the KPF carcinoma are not, we hypothesized that these TNT-derived mNECs are neural-like progenitor cells (NRPs) found in human PDA. In human PDA, NRPs correlate with poor survival and drug resistance [22]. Initially, we asked if our TNT mNECs persist in frank carcinoma, as NRPs do in patients. To test this, we extended the trace time post-tamoxifen treatment to 12 weeks and examined tdTom expression in areas of undifferentiated carcinoma, confirmed by histology (data not shown). As expected, tuft cells were absent in regions of carcinoma, as indicated by IHC for Dclk1 (Fig. 5A, *Left*). However, when we stained adjacent sections for tdTom, we easily found mTC progeny cells scattered throughout the tumors (Fig. 5A, *Right*). Using co-IF, we confirmed that the identity of these mTC progeny were indeed Syp-expressing mNECs (Fig. 5B). We conclude that not only are mTCs undergoing TNT, but the mTC-derived mNECs persist within dedifferentiated carcinoma, consistent with NRPs in PDA patients [20].

TNT gives rise to Nrxn3^{+} neural-like progenitor cells in pancreatic carcinoma

Neurexin 3 (Nrxn3) is a marker of NRPs linked with poor prognosis and chemotherapy resistance in multiple cancers, including colorectal, lung, and pancreatic cancer [20, 31, 32]. The persistence of mNECs in carcinoma led us to examine the expression of Nrxn3 in the TNT-derived mNECs in the KPF carcinoma model. KF neoplasia and KPF carcinoma tissues were co-stained with anti-Nrxn3, anti-Syp, and anti-PanCK to distinguish mNECs with an NRP identity. As expected, *KF-P2f3T* EECs did not express Nrxn3 (Fig. 6A and 6B, *Top*).

However, in the *KPF-P2f3T* carcinoma model, Nrxn3, Syp, and PanCK co-localization confirmed that TNT-derived mNECs cells were indeed NRPs in both areas of neoplasia (Fig. 6A and 6B, *Bottom*) and carcinoma (Fig. 6C).

Targeting cMyc expression specifically to neoplastic mTCs is sufficient to induce transdifferentiation to NRPs

Pancreatic parenchyma-wide expression of *cMyc* induces the formation of mNECs in a KC model of neoplasia [22], similar to what has been found in the prostate and lung [33-36]. NRPs in patient samples are marked by high levels of *Myc* activity in cancers of the pancreas and other tissues [20, 22, 33, 34]. We hypothesized that targeting *cMyc* expression specifically to the mTCs of the *KF-P2f3T* neoplasia mouse, where TNT is not otherwise observed, would be sufficient to induce NRP genesis. To accomplish this, we crossed the *cMyc* Cre-dependent overexpression mouse line, ROSA26$^{LSL\text{-}cMyc/+,}$ into the *KF-P2f3T* model (designated KFMOE) (Fig. 7A). We treated these mice with cerulein to induce transformation and mTC genesis, then treated with tamoxifen 3 weeks later to activate the tdTom reporter and induce Myc overexpression specifically in the mTCs. As previously observed, the control *KF-P2f3T* mice had no mTC-derived mNECs. In contrast, we readily found mTC-derived mNEC genesis in KFMOE tissue as early as 3 days post-induction (Fig. 7B, *Yellow arrows*), with a 6-fold increase in the tdTom^{+} mNEC population 7 weeks post-tamoxifen treatment (Fig 7C, *Pink*). Finally, to determine if the mNECs in the KFMOE mice were NRPs, we co-stained tissue 7 weeks post-tamoxifen for Nrxn3, Syp, and tdTom (Fig. 7D). Indeed, we consistently found NRP identity in the neuroendocrine population induced by overexpressing c-Myc in mTCs. Thus, *cMyc* expression targeted to mTCs is sufficient to induce transdifferentiation to NRPs in a neoplasia model where NRPs are not observed otherwise.

Discussion:

Prolonged injury or expression of oncogenic *Kras* leads to acinar-to-ductal metaplasia comprised of 5 different cell types: gastric pit-like cells, gastric chief-like cells, senescent duct cells, metaplastic neuroendocrine cells (mNECs), and metaplastic tuft cells (mTCs) [7]. The functions of these different metaplastic cell types have only begun to be recognized. For instance, while normal tuft cells have been shown to play roles in combatting infection [37] and promote wound healing [11, 28, 38], mTCs appear to suppress pancreatic cancer progression [8, 10], consistent with a tissue repair role in the precancerous stages of progression.

While mTCs have been shown to functionally hinder progression of pancreatic cancer, they have long been theorized also to be a tumor progenitor cell in the pancreas and stomach [11, 28, 39]. Dclk1, a common tuft cell marker, has been identified as a marker of progenitor cells in the pancreas and intestine [11, 28, 40]. Besides Dclk1, mTCs express other stem cell markers such as CD133, CD24 and CD44 [11], which, together with their low proliferation rate [11, 28, 40, 41], support their role as cancer stem cells. Dclk1^{+} mTCs are important for wound healing in the pancreas. Depleting mTCs reduces the rate of redifferentiation of ductal cells back to acinar cells after injury [28, 40]. While, mTCs have been hypothesized to be tumor initiating cells, mTCs diminish as neoplasia progresses to carcinoma [8, 11], an observation that is not consistent with a mandatory role in tumor formation.

Regarding the disappearance of mTCs through progression, three non-mutually exclusive possibilities are evident: 1) given their relatively low proliferation rate, they are simply being outcompeted by the tumor cell population, 2) they are dying, though we find no evidence that mTCs are undergoing apoptotic cell death (Fig. 1F), or 3) they are changing their cellular identity. To test the latter possibility, we engineered a unique model to trace

mTC fate through progression using a dual recombinase system wherein we could initiate pancreatic transformation using a FlpO driver and the expression of a *tdTomato* lineage tracer, driven by the TC-specific inducible Pou2f3^{CreER} driver. Surprisingly, what we found was that mTCs are stable in *Kras*^{G12D}-driven neoplasia but transdifferentiate to a mNEC identity in *Kras*^{G12D}; *Tp53*$^{+/-}$ carcinoma.

Pancreatic tumor cells expressing neural/neuroendocrine markers have recently been identified in human PDA and are comprised of two different subsets: neuroendocrine-like or enteroendocrine cells (EECs) and neural-like progenitor cells (NRPs), the latter of which is associated with poor outcome. EECs express hormone markers normally confined to islet cells [16, 20, 21], whereas NRPs express markers of neural progenitors, including Nrxn3. We found that mNECs in *Kras*^{G12D}-driven neoplasia arise independent of mTCs and take on an islet-hormone positive EEC identity (Fig. 4), consistent with previous data showing EECs in metaplasia are independent of mTCs and do not depend on *Pou2f3* to develop [21]. In contrast, the majority of the mNECs in *Kras*^{G12D}*; Trp53*$^{+/-}$ carcinoma do derive from mTCs and have an Nrxn3^{+} NRP phenotype (Fig. 6).

Mouse mNECs (both EECs and NRPs) derive from acinar cells [16, 21, 22], but NRPs derive from an mTC intermediate. In patients, NRPs are associated with high *cMyc* expression in PDA and other carcinomas [20, 22, 33, 34]. Supporting the orthologous nature of our mouse NRP cells, we found that targeting *cMyc* expression specifically to mTCs in our neoplasia model was indeed sufficient to drive TNT (Fig. 7). Consistent with their association with poor outcome, we found that murine NRPs are long-lived and persist within undifferentiated carcinomas (Fig. 5 & Fig. 6). Even so, we have not yet observed conditions under which murine NRPs proliferate to constitute a significant population within these carcinomas. Interestingly, it has been shown that NRPs are resistant to chemotherapy and

may be selected for, and possibly proliferate, when confronted with treatment [20], a possibility currently under investigation.

In summary, our study brings us closer to understanding the function and fates of metaplastic tuft cells in pancreatic cancer. When the pancreas undergoes prolonged damage, mTCs develop in metaplastic lesions [9, 11, 23] and are able to assist in healing and regeneration of the pancreas [11, 28]. This tissue repair function appears to be maintained in mouse neoplasia models, where mTCs inhibit the recruitment of immunosuppressive immune cells, thus hindering progression to carcinoma, an effect that is eventually overcome by other neoplastic epithelia [8, 10]. As the epithelial compartment progresses, mTCs that develop mutations in *Trp53* and an associated upregulation of *Myc* [42-44], undergo what we now call a tuft-to-NRP transition [22, 33-35], making mTCs a tumor progenitor cell, of a sort. NRPs, in turn, resist chemotherapy and are associated with worse outcomes and recurrence in PDA [20, 22]. We conclude that, as a result of this unexpected transdifferentiation event, mTCs switch from a tumor suppressive role in early stages to significant contributor to tumor aggressiveness.

Methods

Mouse Models

mTC Lineage tracing

Pou2f3$^{CreERT/+}$ [18], *ROSA26*$^{LSL\text{-}TdTomato/+}$ [26]. These were combined to generate *Ptf1a*$^{FlpO/+}$; *FSF-KRAS*$^{G12D/+}$ [17, 45]; *Pou2f3*$^{CreERT/+}$ [18]; *ROSA26*$^{LSL\text{-}TdTomato/+}$ (*KF-P2f3T*) and *Ptf1a*$^{FlpO/+}$; *FSF-KRAS*$^{G12D/+}$; *Trp53*$^{Frt\text{-}Exons\ 2\ to\ 5\text{-}Frt/+}$ [17, 45]; *Pou2f3*$^{CreERT/+}$ [18]; *ROSA26*$^{LSL\text{-}TdTomato/+}$ (*KPF-P2f3T*) mice. We induced pancreatic damage in the 8- to 9-week-old *KF-P2f3T* mice with a once-daily intraperitoneal injection of cerulein (46-1-50; American Peptide Company,

Inc, Sunnyvale, CA) at a dose of 250 µg/kg for a total of five days. To induce recombination of ROSA26$^{LSL\text{-}TdTomato/+}$ in *KF-P2f3T* and *KPF-P2f3T* models, 11- to 12-week-old mice were treated with 5mg of Tamoxifen (T5648; Millipore-Sigma, St Louis, MO) via oral gavage, once a day, for 5 days. Tamoxifen was dissolved in corn oil before treating mice. Pancreata were then harvested 1-day post-tamoxifen, three days post-tamoxifen, and seven weeks post-tamoxifen to capture different stages of PDA in mice.

Acinar-derived mTCs and mNECs

Ptf1a^{Cre+}*; LSL-KRAS*$^{G12D/+}$*; LSL-Trp53*$^{R172H/+}$*; ROSA26*$^{LSL\text{-}YFP/+}$ [9] were combined to generate KCY and KPCY mice to allow lineage trace of epithelial compartment. KCY mice were treated with Cerulein at 9 weeks old and allowed to recover for 3 weeks. KCY and KPCY mice were treated with Tamoxifen to induce YFP expression in Ptf1a+ cells at twelve weeks of age.

mTC Ablation

A homozygous CreERT knock-in inserted into the *Pou2f3* locus was used to induce metaplastic tuft cell ablation in KF and KPF mice. 8- to 9-week-old *Ptf1a*$^{FlpO/+}$*; FSF-KRAS*$^{G12D/+}$ [17, 45]*; Pou2f3*$^{CreERT/CreERT}$ (KF; Pou2f3$^{CreERT/CreERT}$) mice were treated with cerulein via intraperitoneal injection at a dose of 250 µg/kg for a total of 5 days to induce pancreatic damage. *Ptf1a*$^{FlpO/+}$*; FSF-KRAS*$^{G12D/+}$*; Trp53*$^{Frt\text{-}Exons\ 2\ to\ 5\text{-}Frt/+}$*;* [17, 45] *Pou2f3*$^{CreERT/CreERT}$ (KPF; Pou2f3$^{CreERT/CreERT}$) did not require cerulein to cause damage. Pancreata were harvested at 12 weeks of age to determine ablation of mTCs in both models.

cMyc overexpression in mTCs

To Investigate the role of *cMyc* in the transdifferentiation of mTCs into mNECs, we bred mouse lines to create the genotype: *Ptf1a*$^{FlpO/+}$, *KRAS*$^{FSF\text{-}G12D/+}$, *Trp53*$^{Frt\text{-}Exons\ 2\ to\ 5\text{-}Frt/+}$ [17, 45], *Pou2f3*$^{CreERT/+}$ [14, 19], *ROSA26*$^{LSL\text{-}TdTomato/+}$, *ROSA26* $^{LSL\text{-}cMyc/+}$ [22]. These were combined to generate KFMOE mice comprised of *Ptf1a*$^{FlpO/+}$; *FSF-KRAS*$^{G12D/+}$ [17, 45]; *Pou2f3*$^{CreERT/+}$ [19]; *ROSA26*$^{LSL\text{-}TdTomato/+}$; *ROSA26* $^{LSL\text{-}cMyc/+}$ [22]. KFMOE mice overexpressed *cMyc* and tdTomato reporter specifically in mTCs in the KF neoplasia model. Pancreatic damage was induced in 8- to 9-week-old KFMOE mice with a once-daily intraperitoneal injection of cerulein (46-1-50; American Peptide Company, Inc, Sunnyvale, CA) at a dose of 250 µg/kg for a total of 5 days. To induce recombination of *ROSA26*$^{LSL\text{-}TdTomato/+}$ and *ROSA26*$^{LSL\text{-}cMyc/+}$ [22] in the KFMOE model, eleven- to twelve-week-old mice were treated with 5mg of Tamoxifen (T5648; Millipore-Sigma, St Louis, MO) via oral gavage, once a day, for 5 days. Tamoxifen was dissolved in corn oil before treating mice. We harvested pancreata 3 days post-tamoxifen and seven weeks post-tamoxifen to investigate the role of *cMyc* in mTC-derived mNECs.

Immunohistochemistry (IHC)

Mouse pancreas tissues were fixed overnight in a Z-fix solution (NC9050753; Anatech Ltd, Battle Creek, MI). The pancreas tissues were processed using a Leica ASP300S tissue processor (Buffalo Grove, IL). Sections (4 µm) of paraffin-embedded tissue were stained for target proteins (Table 1) of interest using the Discovery Ultra XT auto Stainer (Ventana Medical Systems Inc, Tucson, AZ). IHC slides were imaged and stitched together by a 3DHisTech scanner (Perkin Elmer, Seattle, WA) using a ×20 objective lens.

Immunofluorescence (IF)

Tissues were prepared as Z-fixed paraffin-embedded blocks, as stated above. In increased dilutions, sectioned tissue was deparaffinized using xylene and a series of ethanol. We boiled the slides in a pH 6.0 Citrate buffer solution for 5 minutes. Slides were allowed to cool at room temperature for 20 mins, then washed in 0.1% tritonX + PBS solution for 15 mins three times for a total of 45 mins. The sections were then blocked in a donkey block solution of 5% donkey serum/1% bovine serum albumin (BSA) in PBS for 1 hour. Following the block, sections were incubated overnight with primary antibodies, as stated in **Supp. Table 1.** The following day, we washed in a 0.1% TritonX + PBS solution for 15 mins thrice. Then Alexa Fluor-conjugated secondary antibodies (1:500, Invitrogen, Carlsbad, CA) were added and incubated at RT for 1hr in the dark. Slides were then washed once more with 0.1% TritonX + PBS + Hoechst 33342 (62249, 1:10000, Thermo Scientific, Carlsbad, CA) solution for 15 mins thrice to remove excess secondary and label nuclei. Lastly, slides were briefly rinsed in deionized water, mounted with Prolong Diamond antifade mountant (P36961; Fisher), and dried overnight at room temperature before imaging.

EdU Proliferation Assay:

The “Click-iT™ Plus EdU Cell Proliferation Kit for Imaging, Alexa Fluor™ 488 dye” (ThermoFisher, Catalog number: C10637) was used to label cells that have undergone proliferation for a specific time period [46]. We dissolved EdU in PBS to a concentration of 1mg/mL. *KPF-P2f3T* mice were treated with tamoxifen at 11- to 12- weeks of age once daily for 5 days. Mice were treated with 100uL of EdU injected via I.P. injection every 12 hours for 3 days post tamoxifen labeling. We harvested the pancreata from each mouse the following morning. We fixed and stained each pancreas as mentioned in the IF protocol above just

until after secondary antibodies were added and washed in 0.1% TritonX + PBS + Hoechst 33342 (62249, 1:10000, Thermo Scientific, Carlsbad, CA) solution for 15 mins three times to removed excess secondary and label nuclei. We detected EdU by making a cocktail using the following components provided by the kit: 440uL of 1x Click-iT Reaction buffer, 10uL of Copper Protectant, 1.2uL of Alexa Fluor Picolyl, and 50uL of Reaction buffer additive. Reagents must be added in the order listed. 100uL of the cocktail was added to each slide and incubated for 30 minutes before washing with 3% BSA in PBS. We rinsed the slides with ddH2O, mounted them with Prolong Diamond antifade mountant (P36961; Fisher), and dried them overnight at room temperature before imaging.

Quantification

HALO Software (Indica Labs, Corrales, NM) was used to quantify whole tissue scanned sections. Quantification excluded blood vessels, lymph nodes, and adipose/connective tissue. We took multiple sections from each tissue throughout the block and averaged them to produce a data point. Through this software, we can train the algorithm to recognize specific areas of tissue and allow us to determine marker expression in different regions of the pancreas using the whole section. We did image analysis as per Indica Labs' recommendations.

Acknowledgements

The authors would like to thank Marina Pasca di Magliano for helpful discussions. This work was supported by R01CA235141, U01CA224145 and U01CA274154 (to HCC). DJSE was supported by the University of Michigan’s Rackham Merit Fellowship, NCI F31CA271576, and NCI T32CA009676. KED is supported by the Vanderbilt Ingram Cancer Center Support Grant (NIH/NCI P30CA068485), the Vanderbilt-Ingram Cancer Center SPORE in

Gastrointestinal Cancer (NIH/NCI P50CA236733), the Vanderbilt Digestive Disease Research Center (NIH/NIDDK P30DK058404), an American Gastroenterological Association Research Scholar Award (AGA2021-13-02), NIH/NIGMS R35GM142709, The Department of Defense (DOD W81XWH2211121), The Sky Foundation, Inc (AWD00000079), and Linda's Hope (Nashville, TN). RCS is supported by: NCI U01CA224012 and R01s CA186241, CA196228 and DoD PA210068. SB was supported by a postdoctoral fellowship from the German Research Foundation (BE 7224/1-1) and a research grant provided by the Sky Foundation. NGS is supported by NCI R00 CA263154 and the Henry Ford Health + Michigan State University Collaboration grant.

References:

1. Society, A.C., *Cancer Facts & Figures 2024.* American Cancer Society, 2024.
2. Chu, L.C., M.G. Goggins, and E.K. Fishman, *Diagnosis and Detection of Pancreatic Cancer.* The Cancer Journal, 2017. **23**(6): p. 333-342.
3. Pihlak, R., J. Weaver, J. Valle, and M. McNamara, *Advances in Molecular Profiling and Categorisation of Pancreatic Adenocarcinoma and the Implications for Therapy.* Cancers, 2018. **10**(1): p. 17.
4. Sahin, I.H., C.A. Iacobuzio-Donahue, and E.M. O'Reilly, *Molecular signature of pancreatic adenocarcinoma: an insight from genotype to phenotype and challenges for targeted therapy.* Expert Opinion on Therapeutic Targets, 2016. **20**(3): p. 341-359.
5. *Pancreatic Cancer: Molecular Characterization, Clonal Evolution and Cancer Stem Cells.* Biomedicines, 2017. **5**(4): p. 65.
6. Benitz, S.*, et al.*, *ROR2 regulates cellular plasticity in pancreatic neoplasia and adenocarcinoma*. 2023, Cold Spring Harbor Laboratory.
7. Schlesinger, Y.*, et al.*, *Single-cell transcriptomes of pancreatic preinvasive lesions and cancer reveal acinar metaplastic cells' heterogeneity.* Nature Communications, 2020. **11**(1).
8. Delgiorno, K.E.*, et al.*, *Tuft Cells Inhibit Pancreatic Tumorigenesis in Mice by Producing Prostaglandin D2.* Gastroenterology, 2020. **159**(5): p. 1866-1881.e8.
9. Delgiorno, K.E.*, et al.*, *Identification and Manipulation of Biliary Metaplasia in Pancreatic Tumors.* Gastroenterology, 2014. **146**(1): p. 233-244.e5.
10. Hoffman, M.T.*, et al.*, *The Gustatory Sensory G-Protein GNAT3 Suppresses Pancreatic Cancer Progression in Mice.* Cellular and Molecular Gastroenterology and Hepatology, 2021. **11**(2): p. 349-369.
11. Bailey, J.M.*, et al.*, *DCLK1 Marks a Morphologically Distinct Subpopulation of Cells With Stem Cell Properties in Preinvasive Pancreatic Cancer.* Gastroenterology, 2014. **146**(1): p. 245-256.
12. Hoover, B., V. Baena, M.M. Kaelberer, F. Getaneh, S. Chinchilla, and D.V. Bohórquez, *The intestinal tuft cell nanostructure in 3D.* Scientific Reports, 2017. **7**(1).
13. Nevo, S., N. Kadouri, and J. Abramson, *Tuft cells: From the mucosa to the thymus.* Immunology Letters, 2019. **210**: p. 1-9.
14. Yamaguchi, T.*, et al.*, *Skn-1a/Pou2f3 is required for the generation of Trpm5-expressing microvillous cells in the mouse main olfactory epithelium.* BMC Neuroscience, 2014. **15**(1): p. 13.
15. Yamashita, J., M. Ohmoto, T. Yamaguchi, I. Matsumoto, and J. Hirota, *Skn-1a/Pou2f3 functions as a master regulator to generate Trpm5-expressing chemosensory cells in mice.* PLOS ONE, 2017. **12**(12): p. e0189340.
16. Ma, Z.*, et al.*, *Single-Cell Transcriptomics Reveals a Conserved Metaplasia Program in Pancreatic Injury.* Gastroenterology, 2022. **162**(2): p. 604-620 e20.
17. Garcia, P.E.*, et al.*, *Differential Contribution of Pancreatic Fibroblast Subsets to the Pancreatic Cancer Stroma.* Cell Mol Gastroenterol Hepatol, 2020. **10**(3): p. 581-599.
18. McGinty, J.W., H.-A. Ting, T.E. Billipp, M.S. Nadjsombati, D.M. Khan, N.A. Barrett, H.-E. Liang, I. Matsumoto, and J. Von Moltke, *Tuft-Cell-Derived Leukotrienes Drive Rapid Anti-helminth Immunity in the Small Intestine but Are Dispensable for Anti-protist Immunity.* Immunity, 2020. **52**(3): p. 528-541.e7.
19. Matsumoto, I., M. Ohmoto, M. Narukawa, Y. Yoshihara, and K. Abe, *Skn-1a (Pou2f3) specifies taste receptor cell lineage.* Nature Neuroscience, 2011. **14**(6): p. 685-687.
20. Hwang, W.L.*, et al.*, *Single-nucleus and spatial transcriptome profiling of pancreatic cancer identifies multicellular dynamics associated with neoadjuvant treatment.* Nature Genetics, 2022. **54**(8): p. 1178-1191.
21. Caplan, L.R., V. Vavinskaya, D.G. Gelikman, N. Jyotsana, V.Q. Trinh, K.P. Olive, M.C.B. Tan, and K.E. Delgiorno, *Enteroendocrine Cell Formation Is an Early Event in Pancreatic Tumorigenesis.* Frontiers in Physiology, 2022. **13**.

22. Farrell, A.S.*, et al.*, *MYC regulates ductal-neuroendocrine lineage plasticity in pancreatic ductal adenocarcinoma associated with poor outcome and chemoresistance.* Nature Communications, 2017. **8**(1).
23. Wu, C.-Y.C.*, et al.*, *PI3K Regulation of RAC1 Is Required for KRAS-Induced Pancreatic Tumorigenesis in Mice.* Gastroenterology, 2014. **147**(6): p. 1405-1416.e7.
24. Baine, M.K.*, et al.*, *SCLC Subtypes Defined by ASCL1, NEUROD1, POU2F3, and YAP1: A Comprehensive Immunohistochemical and Histopathologic Characterization.* Journal of Thoracic Oncology, 2020. **15**(12): p. 1823-1835.
25. Huang, Y.-H.*, et al.*, *POU2F3 is a master regulator of a tuft cell-like variant of small cell lung cancer.* Genes & Development, 2018. **32**(13-14): p. 915-928.
26. Madisen, L.*, et al.*, *A robust and high-throughput Cre reporting and characterization system for the whole mouse brain.* Nat Neurosci, 2010. **13**(1): p. 133-40.
27. Burclaff, J., S.G. Willet, J.B. Sáenz, and J.C. Mills, *Proliferation and Differentiation of Gastric Mucous Neck and Chief Cells During Homeostasis and Injury-induced Metaplasia.* Gastroenterology, 2020. **158**(3): p. 598-609.e5.
28. Westphalen, C.B.*, et al.*, *Dclk1 Defines Quiescent Pancreatic Progenitors that Promote Injury-Induced Regeneration and Tumorigenesis.* Cell Stem Cell, 2016. **18**(4): p. 441-455.
29. Worthington, J.J., F. Reimann, and F.M. Gribble, *Enteroendocrine cells-sensory sentinels of the intestinal environment and orchestrators of mucosal immunity.* Mucosal Immunology, 2018. **11**(1): p. 3-20.
30. Riedel, M.J., A. Asadi, R. Wang, Z. Ao, G.L. Warnock, and T.J. Kieffer, *Immunohistochemical characterisation of cells co-producing insulin and glucagon in the developing human pancreas.* Diabetologia, 2012. **55**(2): p. 372-381.
31. Hu, L.*, et al.*, *Genome-Wide Association Study of Prognosis in Advanced Non–Small Cell Lung Cancer Patients Receiving Platinum-Based Chemotherapy.* Clinical Cancer Research, 2012. **18**(19): p. 5507-5514.
32. Lim, U.*, et al.*, *Susceptibility variants for obesity and colorectal cancer risk: The multiethnic cohort and PAGE studies.* International Journal of Cancer, 2012. **131**(6): p. E1038-E1043.
33. Ireland, A.S.*, et al.*, *MYC Drives Temporal Evolution of Small Cell Lung Cancer Subtypes by Reprogramming Neuroendocrine Fate.* Cancer Cell, 2020. **38**(1): p. 60-78.e12.
34. Lee, J.K.*, et al.*, *N-Myc Drives Neuroendocrine Prostate Cancer Initiated from Human Prostate Epithelial Cells.* Cancer Cell, 2016. **29**(4): p. 536-547.
35. Mollaoglu, G.*, et al.*, *MYC Drives Progression of Small Cell Lung Cancer to a Variant Neuroendocrine Subtype with Vulnerability to Aurora Kinase Inhibition.* Cancer Cell, 2017. **31**(2): p. 270-285.
36. Yin, Y.*, et al.*, *N-Myc promotes therapeutic resistance development of neuroendocrine prostate cancer by differentially regulating miR-421/ATM pathway.* Molecular Cancer, 2019. **18**(1).
37. Howitt, M.R.*, et al.*, *Tuft cells, taste-chemosensory cells, orchestrate parasite type 2 immunity in the gut.* Science, 2016. **351**(6279): p. 1329-1333.
38. Barker, N., *Adult intestinal stem cells: critical drivers of epithelial homeostasis and regeneration.* Nature Reviews Molecular Cell Biology, 2014. **15**(1): p. 19-33.
39. Saqui-Salces, M., T.M. Keeley, A.S. Grosse, X.T. Qiao, M. El-Zaatari, D.L. Gumucio, L.C. Samuelson, and J.L. Merchant, *Gastric tuft cells express DCLK1 and are expanded in hyperplasia.* Histochemistry and Cell Biology, 2011. **136**(2): p. 191-204.
40. Nakanishi, Y.*, et al.*, *Dclk1 distinguishes between tumor and normal stem cells in the intestine.* Nature Genetics, 2013. **45**(1): p. 98-103.
41. May, R.*, et al.*, *Identification of a novel putative pancreatic stem/progenitor cell marker DCAMKL-1 in normal mouse pancreas.* Am J Physiol Gastrointest Liver Physiol, 2010. **299**(2): p. G303-10.
42. Dai, M.-S., Y. Jin, J.R. Gallegos, and H. Lu, *Balance of Yin and Yang: Ubiquitylation-Mediated Regulation of p53 and c-Myc.* Neoplasia, 2006. **8**(8): p. 630-644.
43. Feng, Y.C.*, et al.*, *c-Myc inactivation of p53 through the pan-cancer lncRNA MILIP drives cancer pathogenesis.* Nature Communications, 2020. **11**(1).

44. Ho, J.S.L., W. Ma, D.Y.L. Mao, and S. Benchimol, *p53-Dependent Transcriptional Repression of c-myc Is Required for G₁ Cell Cycle Arrest.* Molecular and Cellular Biology, 2005. **25**(17): p. 7423-7431.
45. Wu, J.*, et al.*, *Generation of a pancreatic cancer model using a Pdx1-Flp recombinase knock-in allele.* PLOS ONE, 2017. **12**(9): p. e0184984.
46. Zhang, H.*, et al.*, *Glucose-Mediated Repression of Menin Promotes Pancreatic β-Cell Proliferation.* Endocrinology, 2012. **153**(2): p. 602-611.

Figure Legends:

Figure 1. Lineage trace model shows tuft cell specific expression of tdTomato.

Genetic strategy to trace the fate of metaplastic tuft cells (mTCs) in pancreatic cancer progression using a dual recombinase neoplasia (*KF-P2f3T*) model **(A)** and carcinoma (*KPF-P2f3T*) model **(B)**. **C)** Treatment regimen for neoplasia and carcinoma Models. The models have both pancreatic progression and reporter specifically in tuft cells. The *KF-P2f3T* model utilizes Cerulein once daily, follow by 2 weeks recovery, then once daily tamoxifen treatment for 5 days. The *KPF-P2f3T* model is aggressive as it contains one null p53 allele. Cerulein is not necessary and so only Tamoxifen is treated once daily for 5 days. Mice are allowed to age for different time points to determine lineage of metaplastic tuft cells in progression of pancreatic cancer. **D)** Dclk1 in Brown identifies tuft cells in neoplasia model (left) and carcinoma model (right). **E)** Specific expression of tdTomato reporter in both models. White represents Hoechst staining to mark the nucleus, tdTomato in red to show recombination of tdTomato (tdTom), Pou2f3, the master regulator of tuft cells in Green, and Acetylated alpha tubulin in Magenta to mark filamentous actin in the tufts of the mTCs. **F)** Dual IHC of tdTom (Teal) and CC3 (Brown) stained *KF-P2f3T* and *KPF-P2f3T* mice to determine cell death of mTCs in neoplasia and carcinoma. Black arrows indicate tdTom+ cells in lesions.

Figure 2. Lineage tracing mTCs reveals transdifferentiation to metaplastic neuroendocrine cells (mNECs).

Dual recombinase models show fate of mTCs in progression of pancreatic cancer. **A)** Mice harvested 3 days post-tamoxifen treatment for labeling mTCs. Hoechst stains nucleus of cells (White), Cox1 is used to identify mTCs (Green), tdTom reporter to determine fate of mTCs (Red) and acetylated-α-tubulin (Magenta) marks filamentous actin on tuft of mTCs. **B)** Quantification of Percentage of mTC (Black) and mTC Progeny (Pink) among ductal cells at different time points post-tamoxifen treatment

in *KF-P2f3T* and *KPF-P2f3T* models. mTCs are identified by Cox1 and tdTom, mTC Progeny are only tdTom positive. (n = 3/group) p-values were calculated using a multi-way ANOVA on Prism Graphpad 7. * = $p < 0.05$, ** = $p < 0.01$. **C)** Co-staining of tdTomato (Red) expression with remaining metaplastic ductal cell subsets. In Green, Gkn1, Lectin GS-II, and Synaptophysin (Syp) mark gastric pit-like, gastric neck-like, and neuroendocrine cells respectively in pancreatic metaplastic ducts. **D)** 7 weeks post-tamoxifen labeling of neoplasia and carcinoma models exposes shift of populations. Cox1 (Green) marks mTCs, tdTomato (Red) identifies reporter, Syp (White) marks neuroendocrine cells, and Blue represents DAPI Staining to identify the nucleus of a cell. **E)** Quantification of percentage of mTCs (Cox1+ tdTom+) in Black, mTC-derived mNECs (Syp+ tdTom+) in Pink, mTC-independent mNECs (Syp+ tdTom-) in Green. (n = 3/group). p-values were calculated using a multi-way ANOVA on Prism Graphpad 7. * = $p < 0.05$, ** = $p < 0.01$.

Figure 3. Characterizing the tuft cell to neuroendocrine cell transdifferentiation (TNT).

IF staining of Cox1 (Red) and Syp (Green) in neoplasia and carcinoma models determines that mNECs in the *KPF-P2f3T* model relies on the mTC population. **A)** Cox1 (Red) and Syp (Green) markers are stained in Pou2f3 double knock-in models of pancreatic neoplasia and carcinoma: (Left) KF; Pou2f3$^{CreERT/CreERT}$ and (Right) KPF; Pou2f3$^{CreERT/CreERT}$, correspondingly to investigate the role of tuft cells in mNEC genesis. Green Arrows denote mNECs, Red Asterisks denote stromal Cox1^{+} staining identifying Cox1^{+} Immune cells. **B)** Pou2f3, the master regulator of tuft cells (Cyan) is stained with Cox1, marker of tuft cells (Red), and Syp, neuroendocrine marker (Green) to determine if mNECs also express Pou2f3. **C)** Dual IHC of Syp (Teal) and Ki67 (Brown) of neoplasia and carcinoma models of pancreas to determine proliferation of mNECs. **D)** Co-IF of mTC marker, Cox1 (Green), lineage tracer, tdTom (Red), mNEC marker, Syp (White), incorporated EdU (Magenta) to mark proliferating cells, and nuclear marker, Hoechst (Blue) in *KPF-P2f3T* mice treated with EdU over the course of 3 days post-tamoxifen treatment. **E)** Yellow arrows mark rare transitionary cells that are marked with

both Syp (Green) and Cox1 (Red). Green arrow identifies cells that are only expressing Syp, mNECs. Red arrow marks cells only expressing Cox1, mTCs.

Figure 4. Identifying distinctions between mNECs in the progression of PDA.

Neoplasia and carcinoma PDA models were stained with markers of different islet compartments to determine differences between mNECs between the *KF-P2f3T* and *KPF-P2f3T* models. **B)** Islets and lesions from *KF-P2f3T* and *KPF-P2f3T* are shown to determine co-localization of Syp (Red) and markers of the different compartments of the Islet (Green). PanCK (Cyan) was used to distinguish islet cells from mNECs, and Hoechst was used to mark the nucleus of each cell. Glucagon (Gcg), Insulin (Ins), Somatostatin (Sst), Ghrelin (Ghrl), and Pancreatic Polypeptide (Pp) were stained to identify the α cells, β cells, δ cells, ε cells and γ cells respectively.

Figure 5. mTC-derived mNECs are identified in PDA Carcinoma.

IHC and IF are used to confirm the identity of mTC Progeny in dedifferentiated carcinoma of *KPF-P2f3T* model. **A)** IHC of dedifferentiated carcinoma stained with Dclk1 (*Left*) and tdTomato (*Right*) in Brown. **B)** Dedifferentiated carcinoma of *KPF-P2f3T* model is stained with Hoechst (Cyan), Syp (White), and tdTomato (Red) to determine identity of mTC progeny.

Figure 6. Identification of mTC-derived Nrxn+ NRPs in Carcinoma

Co-staining of Synaptophysin (Red), Nrxn3 (Green), PanCK (Magenta), and Hoechst (White) in *KF-P2f3T* neoplasia model and *KPF-P2f3T* carcinoma model at **A)** 3 days post-tamoxifen, **B)** 7 weeks post-tamoxifen, and **C)** *KPF-P2f3T* dedifferentiated carcinoma.

Figure 7. cMyc Mediated development of mNECs.

Overexpression of cMyc in *KF-P2f3T* model shows dependence of TNT cell development in PDA progression. **A)** Genetic and treatment strategy of tuft cell specific cMyc overexpression and PDA progression known as KFMOE model. **B)** KFMOE 3 days and 7 weeks post-tamoxifen treatment are stained with tdTom (Red), Syp (Green), Acetylated-α-tubulin (Magenta), and Hoechst (White) to identify mTC-derived mNECs in both time points. **C)** Quantification of mTCs (Cox1+ tdTom+) in Black, mTC-derived mNECs (Syp+ tdTom+) in Pink and mTC-independent mNECs (Syp+ tdTom-) in Green for *KF-P2f3T* and KFMOE models. Mice were sac'd after 3 days and 7 weeks post tamoxifen treatment to label tuft cells with tdTomato and overexpress cMyc specifically in tuft cells. (n = 3/group) p-values were calculated using a multi-way ANOVA on Prism Graphpad 7. * = $p < 0.05$. **D)** KFMOE 7wks post-tamoxifen treatment tissue is stained for co-IF to determine expression of Syp (Green), tdTom (Red), Nrxn3 (Magenta), and Hoechst (White).

Figure 1

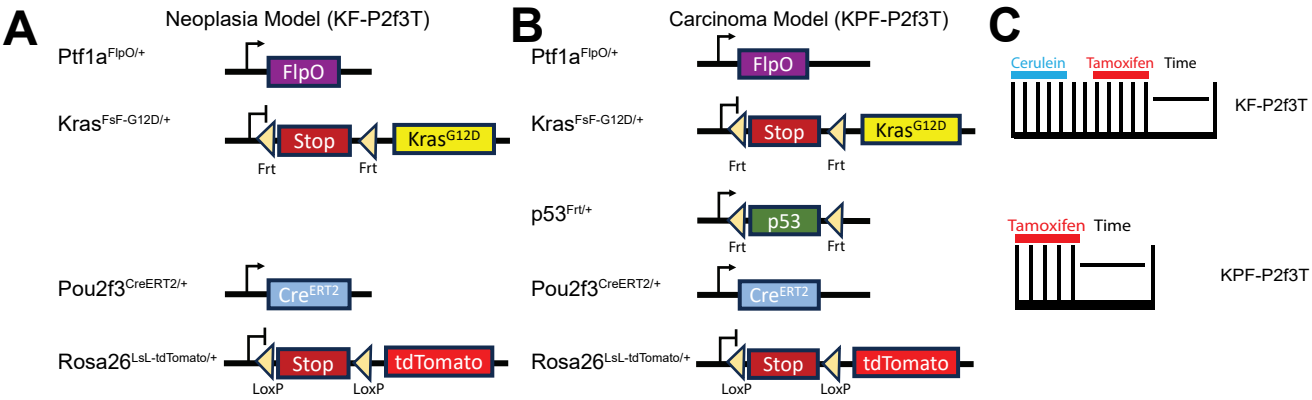
A
Neoplasia Model (KF-P2f3T)
Ptf1a FlpO/+
FlpO
Kras FsF-G12D/+
Stop
Kras G12D
Frt
Frt
Pou2f3 CreERT2/+
Cre ERT2
Rosa26 LsL-tdTomato/+
Stop
tdTomato
LoxP
LoxP
B
Carcinoma Model (KPF-P2f3T)
Ptf1a FlpO/+
FlpO
Kras FsF-G12D/+
Stop
Kras G12D
Frt
Frt
p53 Frt/+
p53
Frt
Frt
Pou2f3 CreERT2/+
Cre ERT2
Rosa26 LsL-tdTomato/+
Stop
tdTomato
LoxP
LoxP
C
Cerulein
Tamoxifen
Time
KF-P2f3T
Tamoxifen
Time
KPF-P2f3T

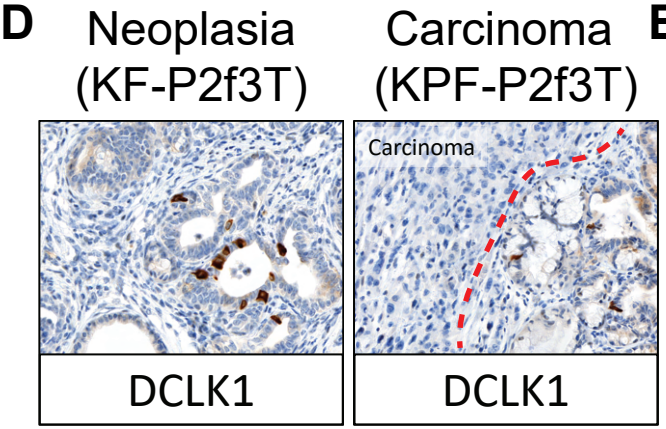
D
Neoplasia (KF-P2f3T)
Carcinoma (KPF-P2f3T)
Carcinoma
DCLK1
DCLK1

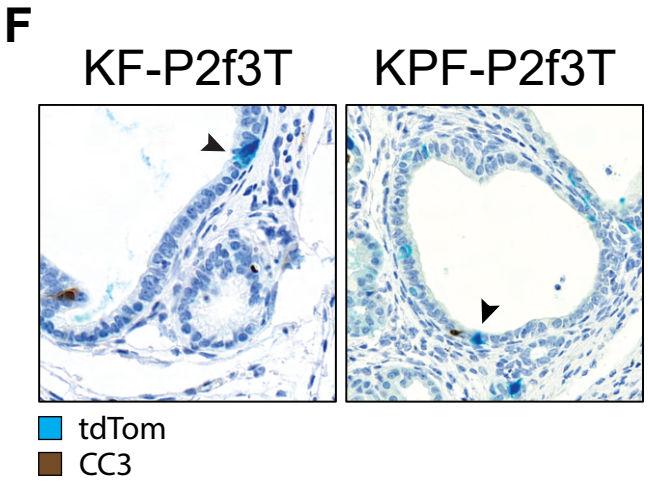
F
KF-P2f3T
KPF-P2f3T
tdTom
CC3

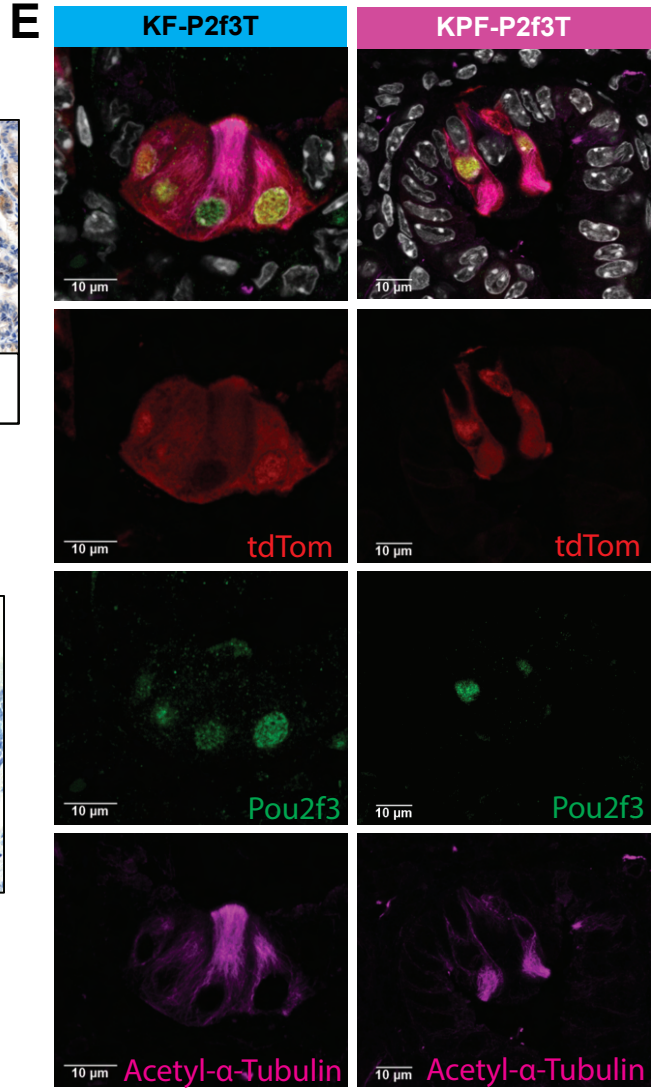
E
KF-P2f3T
KPF-P2f3T
10 µm
tdTom
Pou2f3
Acetyl-α-Tubulin

Figure 2

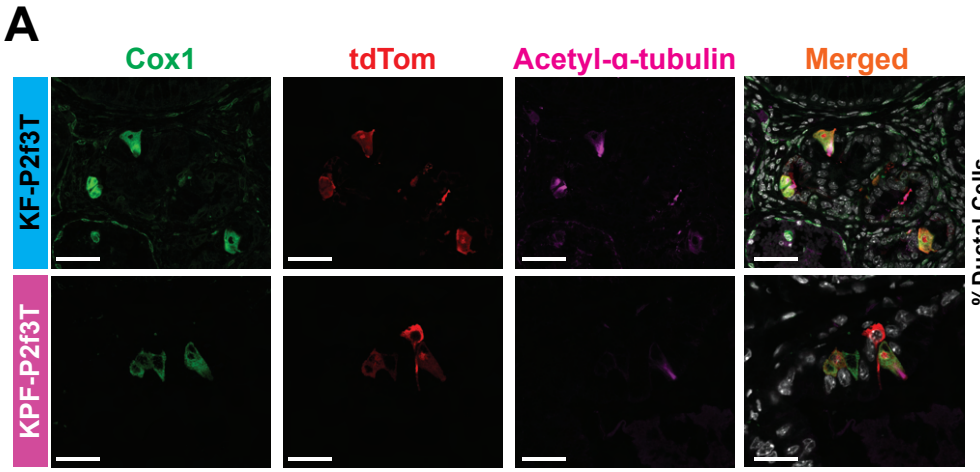
A
Cox1
tdTom
Acetyl-α-tubulin
Merged
KF-P2f3T
KPF-P2f3T

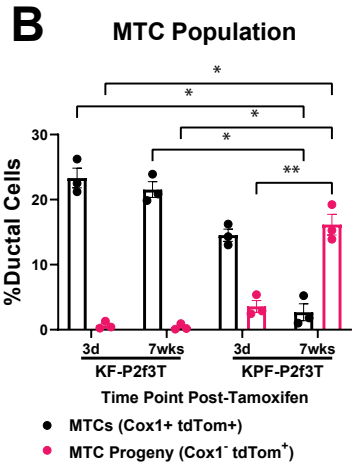
B
MTC Population
%Ductal Cells
0
10
20
30
*
*
*
*
**
3d
7wks
3d
7wks
KF-P2f3T
KPF-P2f3T
Time Point Post-Tamoxifen
MTCs (Cox1+ tdTom+)
MTC Progeny (Cox1- tdTom+)

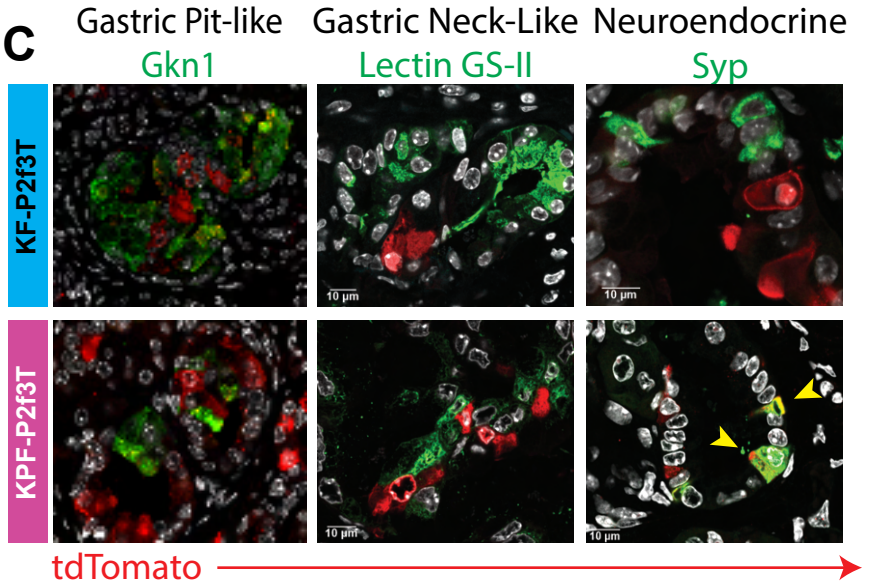
C
Gastric Pit-like
Gastric Neck-Like
Neuroendocrine
Gkn1
Lectin GS-II
Syp
KF-P2f3T
KPF-P2f3T
10 µm
tdTomato

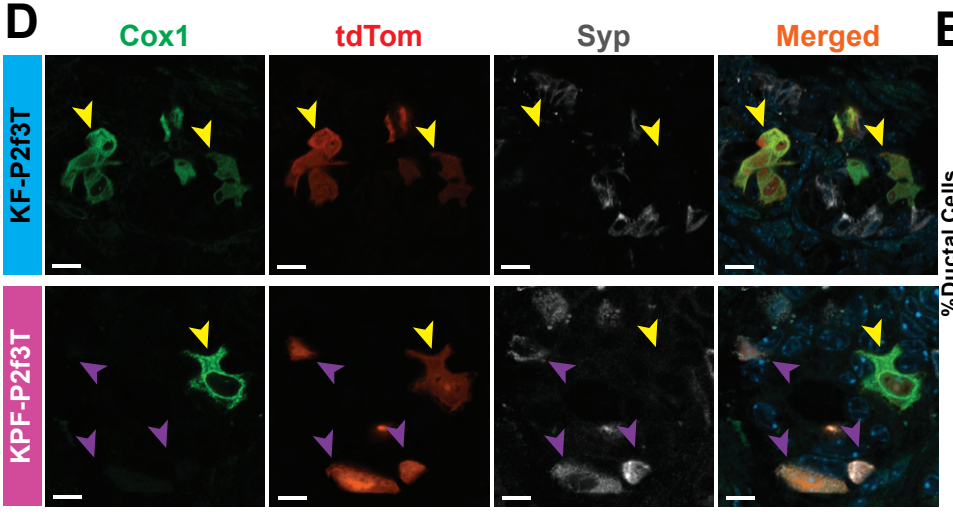
D
Cox1
tdTom
Syp
Merged
KF-P2f3T
KPF-P2f3T

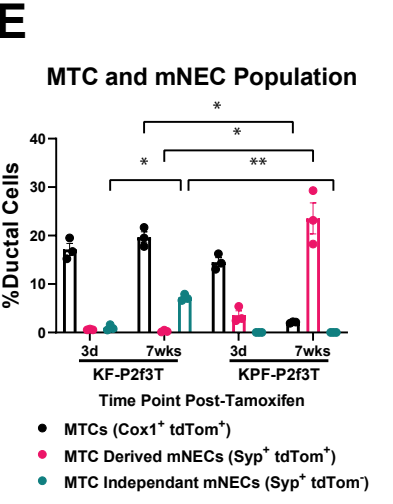
E
MTC and mNEC Population
%Ductal Cells
0
10
20
30
40
*
*
*
**
3d
7wks
3d
7wks
KF-P2f3T
KPF-P2f3T
Time Point Post-Tamoxifen
MTCs (Cox1+ tdTom+)
MTC Derived mNECs (Syp+ tdTom+)
MTC Independant mNECs (Syp+ tdTom-)

Figure 3

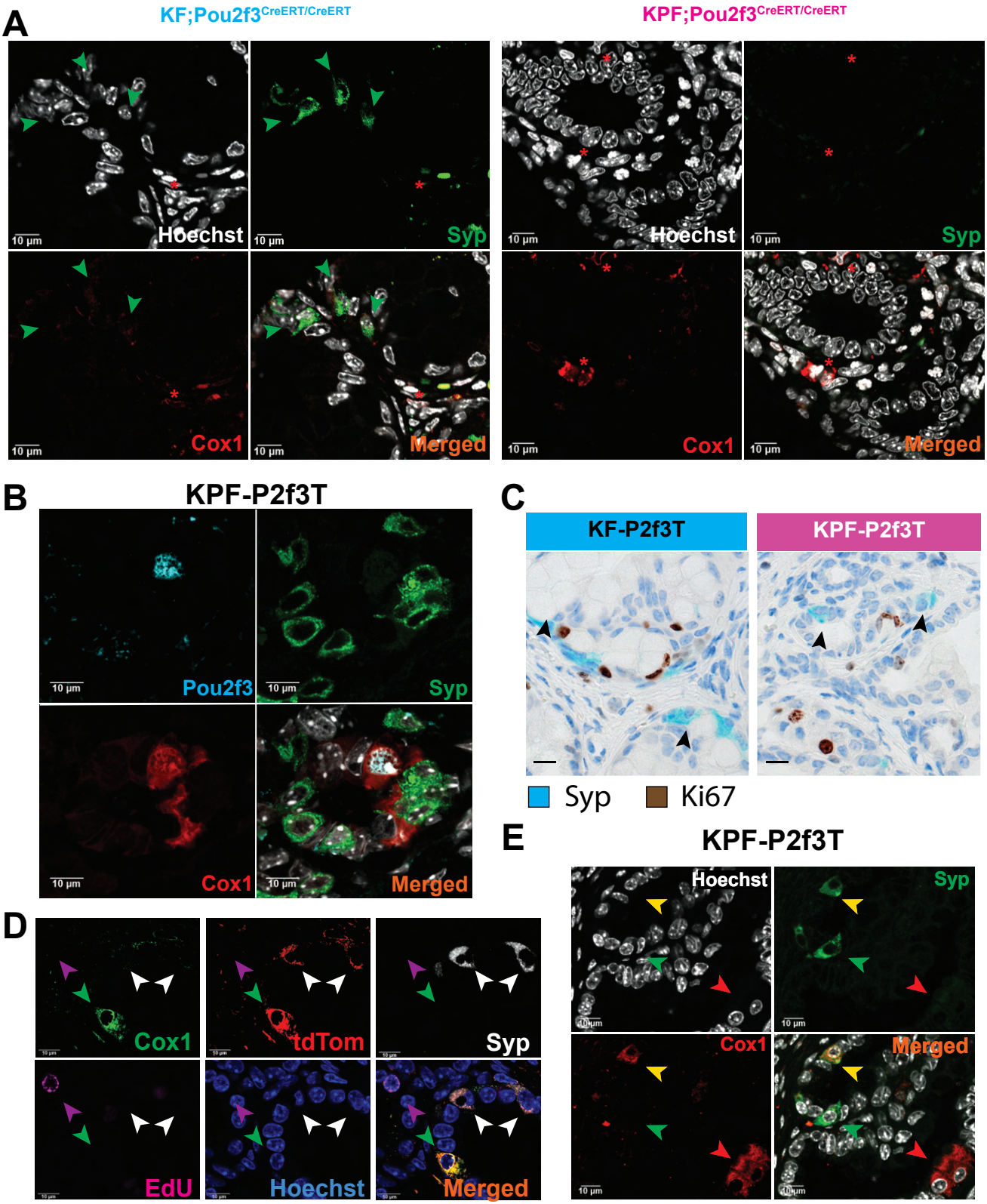
A
KF;Pou2f3CreERT/CreERT
KPF;Pou2f3CreERT/CreERT
Hoechst
Syp
Cox1
Merged
10 µm
B
KPF-P2f3T
Pou2f3
Syp
Cox1
Merged
C
KF-P2f3T
KPF-P2f3T
Syp
Ki67
D
Cox1
tdTom
Syp
EdU
Hoechst
Merged
E
KPF-P2f3T
Hoechst
Syp
Cox1
Merged

Figure 4

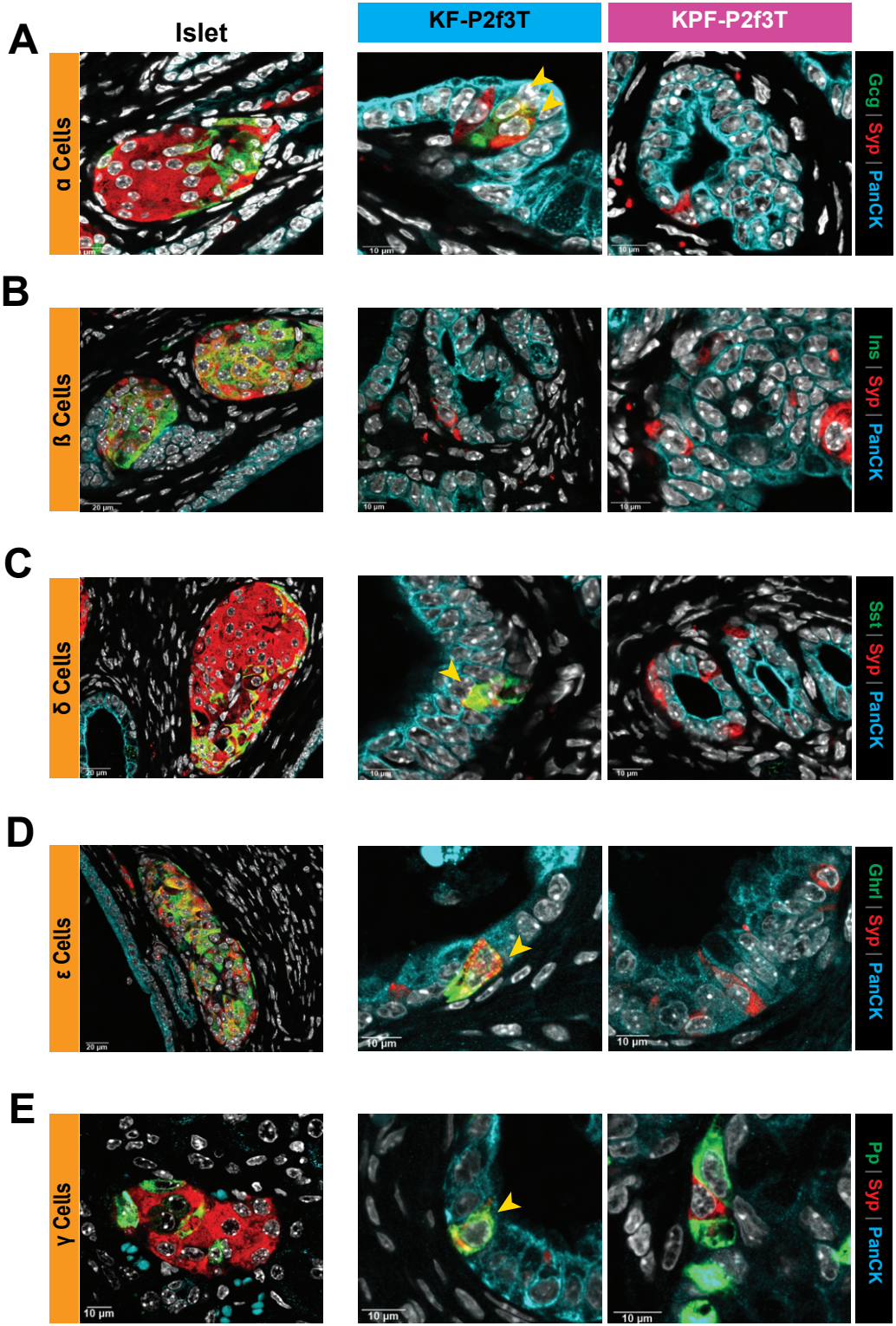
A
Islet
KF-P2f3T
KPF-P2f3T
α Cells
Gcg | Syp | PanCK
B
ß Cells
Ins | Syp | PanCK
C
δ Cells
Sst | Syp | PanCK
D
ε Cells
Ghrl | Syp | PanCK
E
γ Cells
Pp | Syp | PanCK
10 µm

Figure 5

A **KPF-P2f3T**

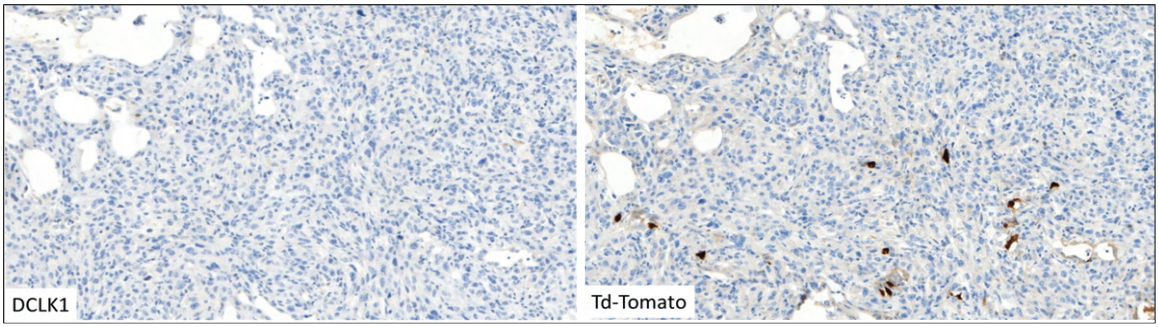

B **KPF-P2f3T**

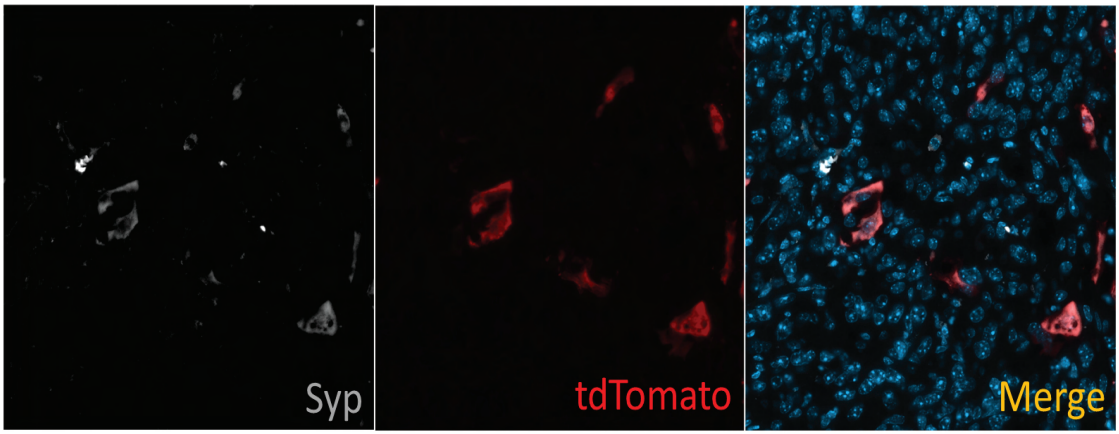

Figure 6

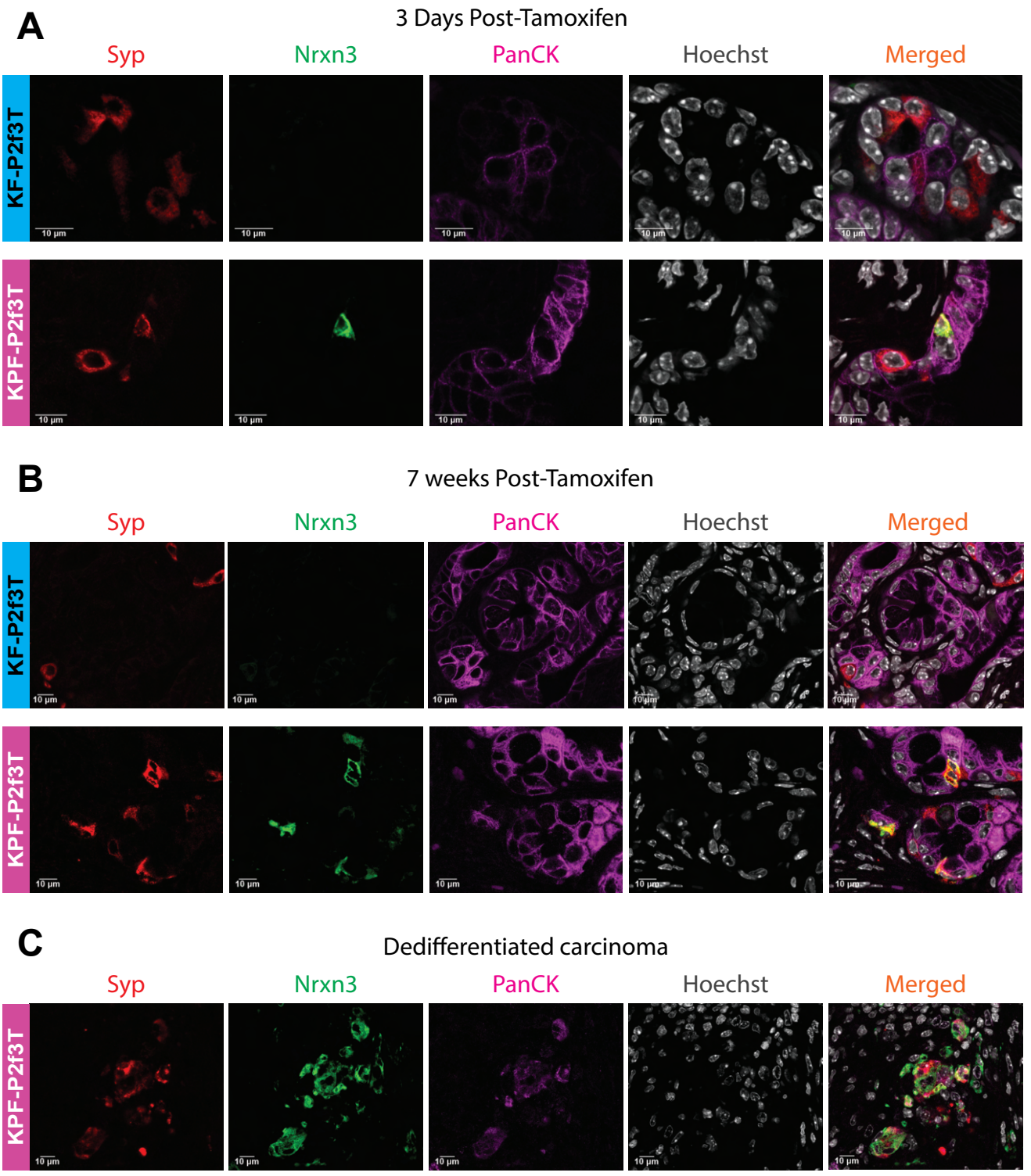
A
3 Days Post-Tamoxifen
Syp
Nrxn3
PanCK
Hoechst
Merged
KF-P2f3T
KPF-P2f3T
10 µm
B
7 weeks Post-Tamoxifen
Syp
Nrxn3
PanCK
Hoechst
Merged
KF-P2f3T
KPF-P2f3T
10 µm
C
Dedifferentiated carcinoma
Syp
Nrxn3
PanCK
Hoechst
Merged
KPF-P2f3T
10 µm

Figure 7

A KFMOE

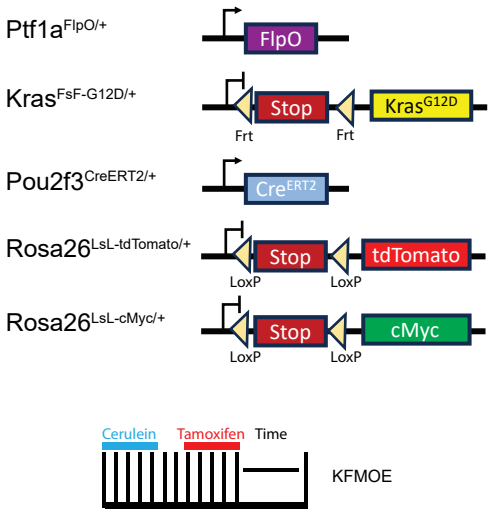

B KFMOE 3 days / KFMOE 7wks

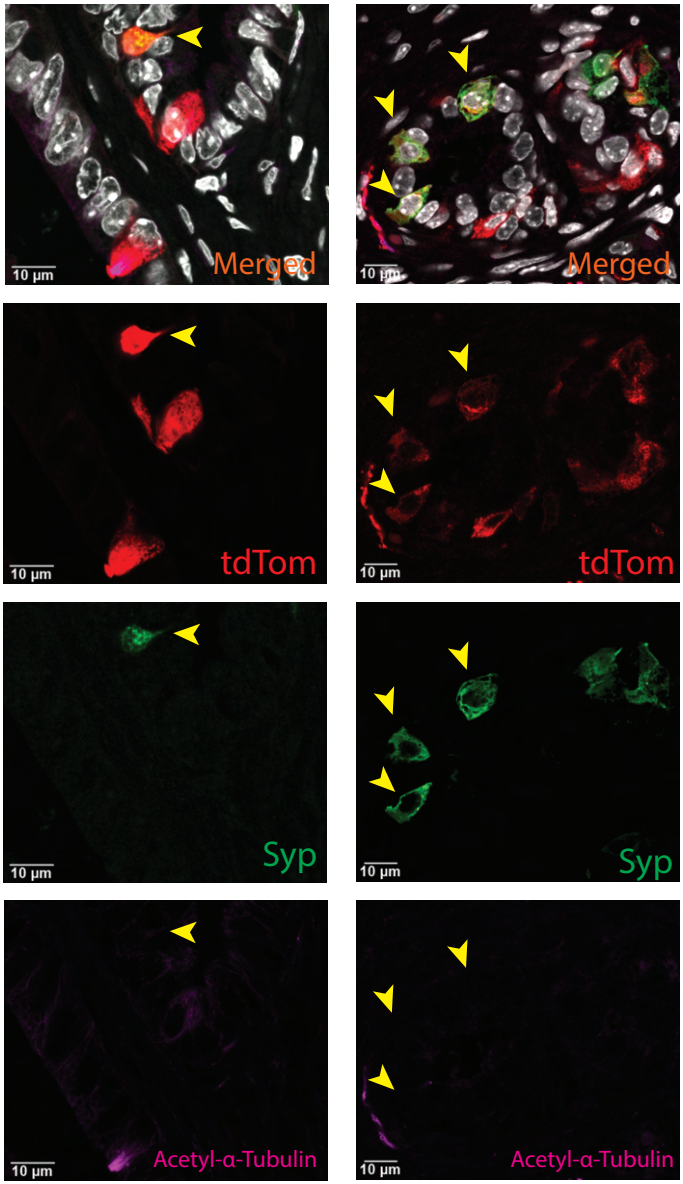

C KF-P2f3T Vs. KFMOE Populations

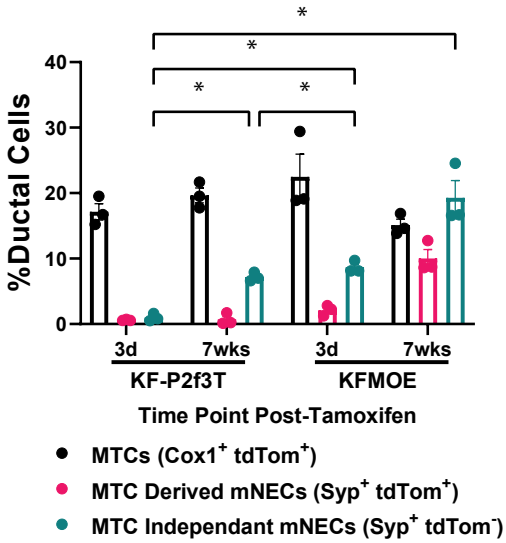
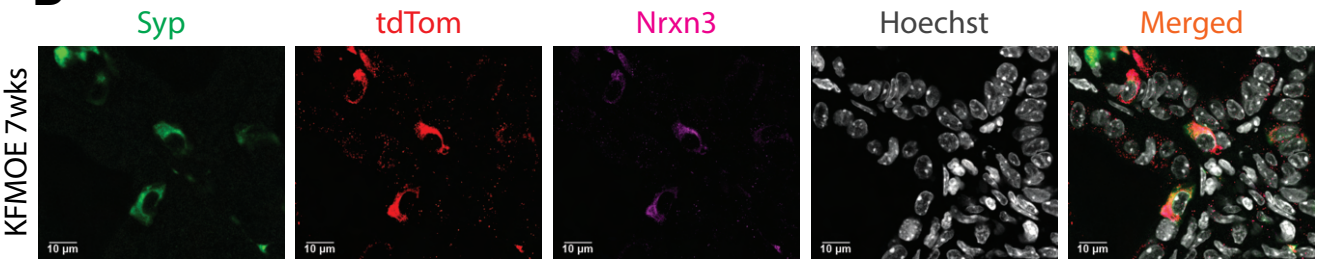
D